

A second-order semi-Lagrangian particle FEM (SL-PFEM) method for the incompressible Navier-Stokes equations

**B. Serván-Camas ^a, J. García-Espinosa ^{a,b},
Jonathan Colom-Cobb ^a**

^a *Centre Internacional de Mètodes Numèrics en Enginyeria (CIMNE), Division of Marine Research, Gran Capitan s/n, 08034 Barcelona, Spain*

^b *Universitat Politècnica de Catalunya, BarcelonaTech (UPC), Campus Nàutica, Edif. NT3, C. Escar 6-8, 08039 Barcelona, Spain*

The International Centre for Numerical Methods in Engineering (CIMNE) is a public research organization created in 1987 at the heart of BarcelonaTech.

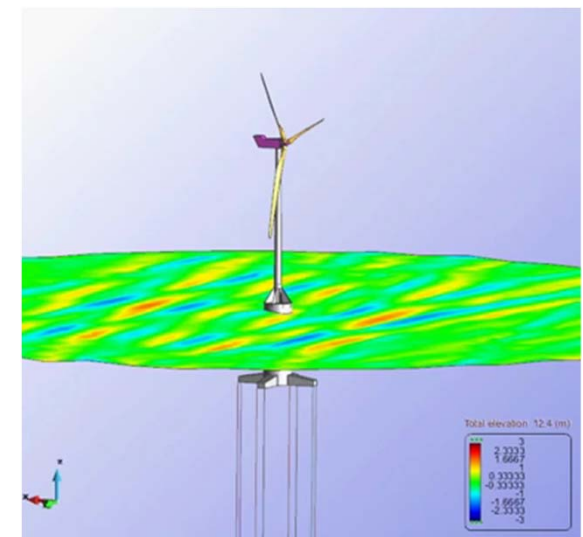
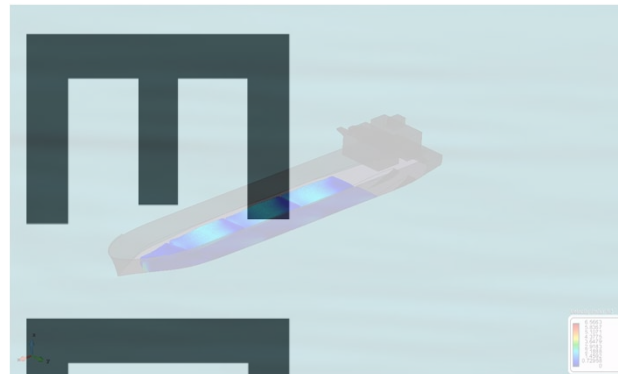
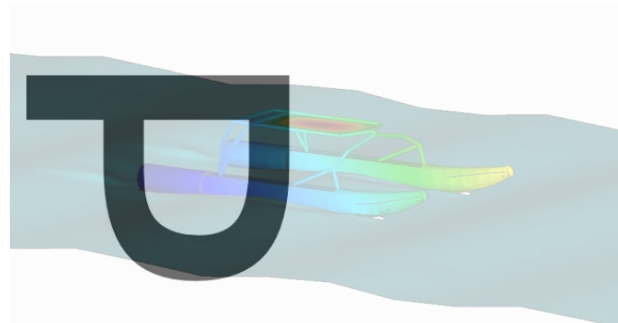
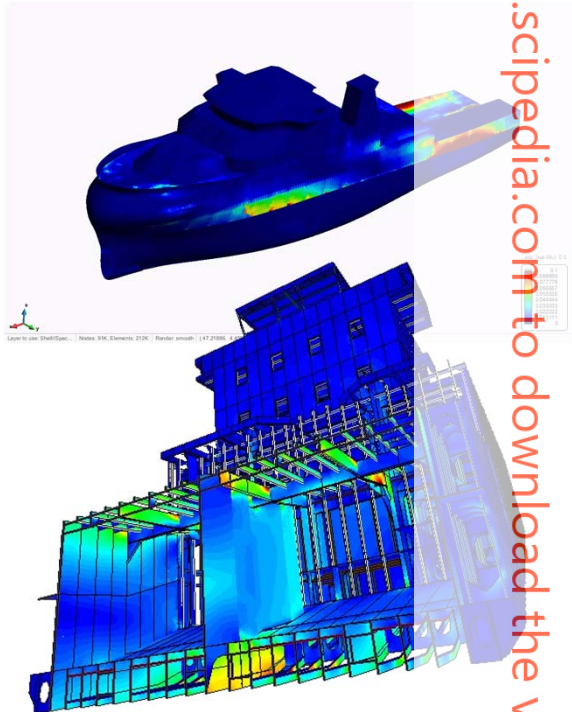
The aim of CIMNE is the development of numerical methods and computational techniques for advancing knowledge and technology in engineering and applied sciences.

CIMNE has received the “Centre for Excellence Severo Ochoa” accreditation (the only one specialized in computational methods in engineering).



CIMNE MARINE is the naval architecture, marine and offshore engineering department of CIMNE:

- Hydrodynamics
- Waves and seakeeping
- Structural and coupled analysis
- Design, assessment and optimization



OUTLINE

1. The SL-PFEM method
 - 1.1 Semi-Lagrangian approach
 - 1.2 SL-PFEM basis
2. Verification and convergence analyses
 - 2.1 Taylor-Green vortex
 - 2.2 Lid driven cavity flow
 - 2.3 3D flow past a cylinder
3. Enriched SL-PFEM
 - 3.1 Free surface flows
 - 3.2 Fluid-Solid interfaces

Acknowledgements



SL-PFEM

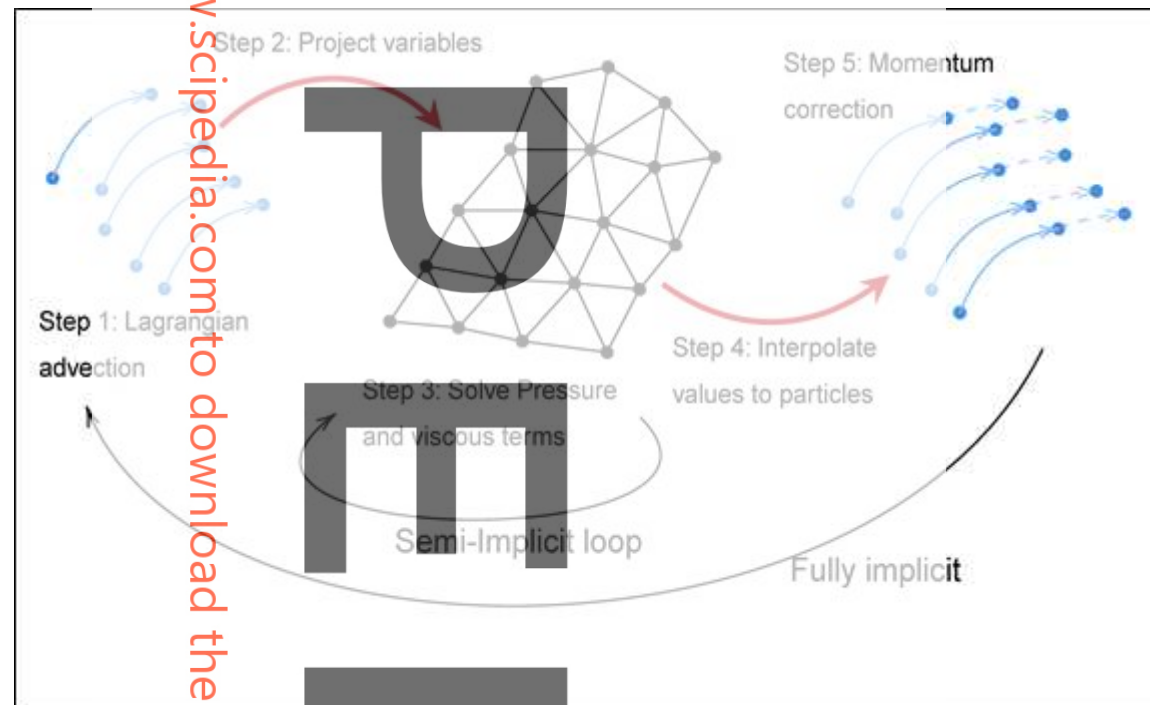
IPED

Register for free at <https://www.sciencedirect.com> to download the version

SEMI-LAGRANGIAN APPROACH

Concepts of the Semi-Lagrangian particle Finite Element Method (SL-PFEM)

First introduced by: S. R. Idesohn, N. Nigro, A. Limache, E. Oñate: Large time-step explicit integration method for solving problems with dominant convection. Computer Methods in Applied Mechanics and Engineering 217-220, 168–185 (2012). DOI 10.1016/j.cma.2011.12. 008.



SEMI-LAGRANGIAN APPROACH

Register for free at <https://www.scipedia.com> to download the version



SEMI-LAGRANGIAN APPROACH

Integrating the particle's equation of motion

Let $\mathbf{a}(\mathbf{x}, t)$ be an acceleration field and let $\{\lambda\}$ be a set of particles each of them identified with a label λ .

Particle's equation of motion:

$$\begin{aligned} \frac{d}{dt} \mathbf{U}_\lambda(t) &= \mathbf{A}_\lambda(t) = \mathbf{a}(\mathbf{X}_\lambda(t), t) \\ \frac{d}{dt} \mathbf{X}_\lambda(t) &= \mathbf{U}_\lambda(t) \end{aligned}$$

Velocity Verlet algorithm:

$$\begin{aligned} \mathbf{X}_\lambda(t^{n+1}) &= \mathbf{X}_\lambda(t^n) + \Delta t \mathbf{U}_\lambda(t^n) + \frac{\Delta t^2}{2} \mathbf{A}_\lambda(t^n) + O(\Delta t^3) \\ \mathbf{U}_\lambda(t^{n+1}) &= \mathbf{U}_\lambda(t^n) + \frac{\Delta t}{2} (\mathbf{A}_\lambda(t^n) + \mathbf{A}_\lambda(t^{n+1})) + O(\Delta t^3) \end{aligned}$$



SL-PFEM for the incompressible Navier-Stokes equations

Let $\mathbf{u}(\mathbf{x}, t)$ be a fluid velocity field and let's define the acceleration field $\mathbf{a}(\mathbf{x}, t)$:

$$\mathbf{a} = d_t \mathbf{u} = \partial_t \mathbf{u} + \mathbf{u} \cdot \nabla \mathbf{u} = -\nabla \left(\frac{P}{\rho} \right) + \nu \Delta \mathbf{u} + \mathbf{f}$$

Move particles (explicit):

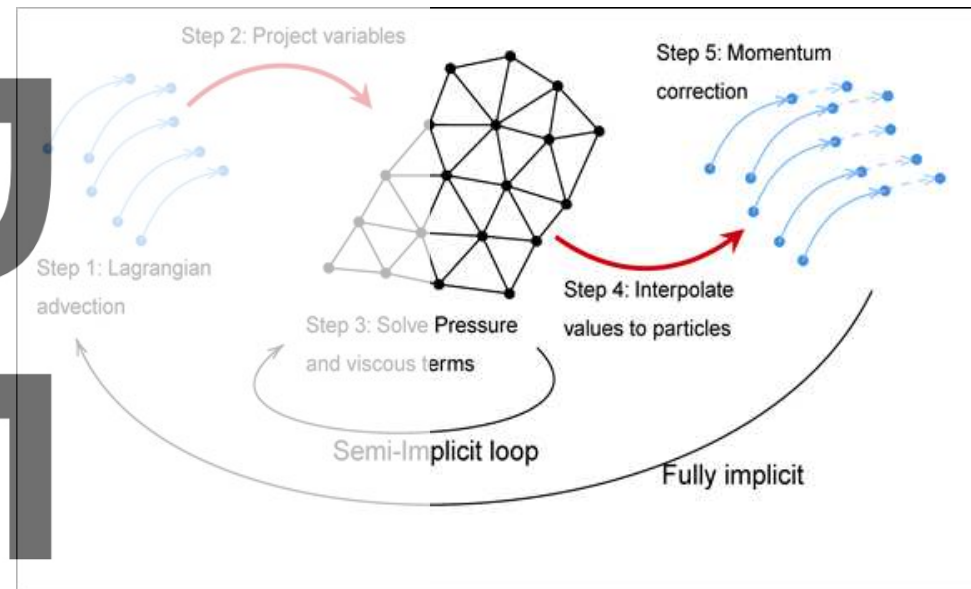
$$\mathbf{X}_\lambda^{n+1} = \mathbf{X}_\lambda^n + \Delta t \mathbf{u}^n(\mathbf{X}_\lambda^n) + \frac{\Delta t}{2} \mathbf{a}^n(\mathbf{X}_\lambda^n)$$

Update velocity (explicit):

$$\mathbf{U}_\lambda^{n+1/2} = \mathbf{U}_\lambda^n + \frac{\Delta t}{2} \mathbf{a}^n(\mathbf{X}_\lambda^n)$$

Correct velocity (implicit):

$$\mathbf{U}_\lambda^{n+1} = \mathbf{U}_\lambda^{n+1/2} + \frac{\Delta t}{2} \mathbf{a}^{n+1}(\mathbf{X}_\lambda^{n+1})$$



SL-PFEM

SL-PFEM for the incompressible Navier-Stokes equations

Projection onto FEM mesh: $\mathbf{u}^{n+1}(\mathbf{x}) = \mathcal{P}_{\{\lambda\}}^{n+1} [\{\mathbf{U}_{\lambda}^{n+1}\}]$:

$$\mathcal{P}_{\{\lambda\}}^{n+1} [\{\mathbf{U}_{\lambda}^{n+1}\}] = \mathcal{P}_{\{\lambda\}}^{n+1} [\{\mathbf{U}_{\lambda}^{n+1/2}\}] + \frac{\Delta t}{2} \mathcal{P}_{\{\lambda\}}^{n+1} [\{\mathbf{a}^{n+1}(\mathbf{X}_{\lambda}^{n+1})\}]$$

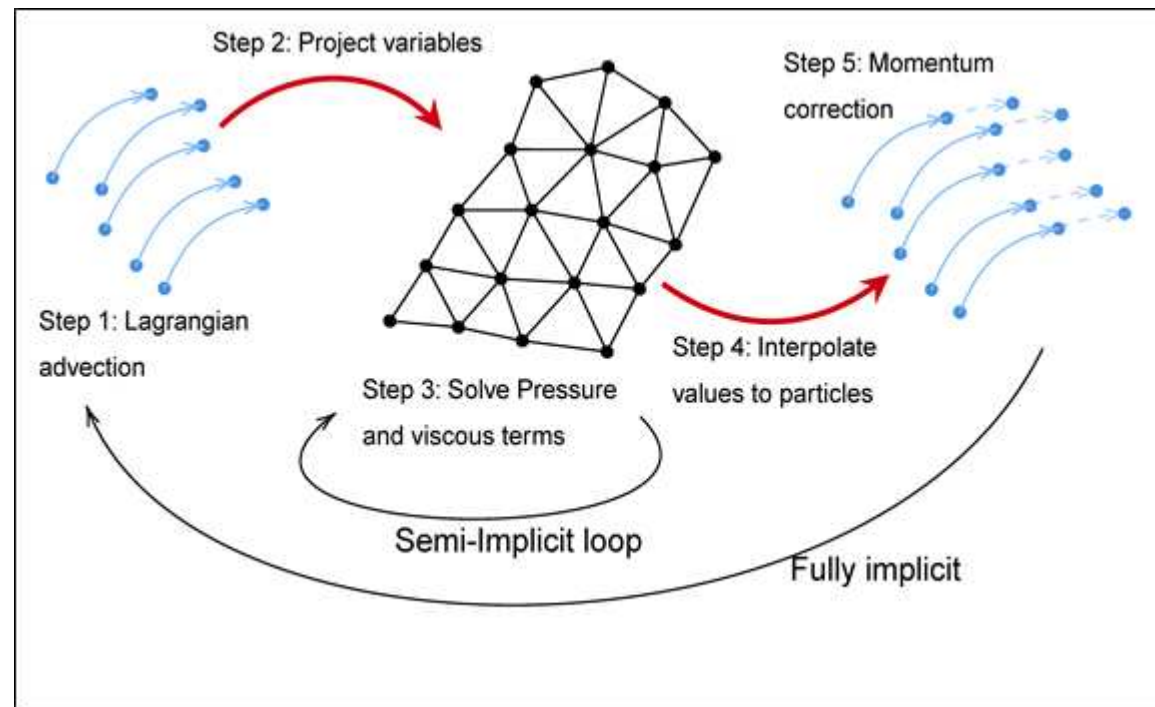
$$\mathbf{u}^{n+1}(\mathbf{x}) = \mathbf{u}_{\mathcal{P}}^{n+1/2} + \frac{\Delta t}{2} \mathcal{P}_{\{\lambda\}}^{n+1} [\{\mathbf{a}^{n+1}(\mathbf{X}_{\lambda}^{n+1})\}]$$

Coherence condition: $\mathbf{a}^{n+1}(\mathbf{x}) = \mathcal{P}_{\{\lambda\}}^{n+1} [\{\mathbf{a}^{n+1}(\mathbf{X}_{\lambda}^{n+1})\}]$

$$\frac{\mathbf{u}^{n+1}(\mathbf{x}) - \mathbf{u}_{\mathcal{P}}^{n+1/2}(\mathbf{x})}{\Delta t} = \frac{1}{2} \mathbf{a}^{n+1}(\mathbf{x})$$

SL-PFEM

SL-PFEM for the incompressible Navier-Stokes equations



Remark: the coherence condition makes it unnecessary to iterate at the outer implicit loop.

SL-PFEM

Semi-Lagrangian approach for the incompressible Navier-Stokes equations

Eulerian description (Stokes' type equation):

$$\frac{\mathbf{u}^{n+1} - \mathbf{u}_{\mathcal{P}}^{n+1/2}}{\Delta t} = \underbrace{\frac{1}{2} \left(-\nabla \left(\frac{p^{n+1}}{\rho} \right) + \nu \Delta \mathbf{u}^{n+1} + \mathbf{f}^{n+1} \right)}_{\mathbf{a}^{n+1}}$$
$$\nabla \cdot \mathbf{u}^{n+1} = 0$$

Solved using FEM implicit scheme inspired in the fractional step method.

SL-PFEM

Semi-Lagrangian approach for the incompressible Navier-Stokes equations

FEM scheme inspired in the fractional step method):

$$v = 0 \text{ (Non-iterative):} \quad \bar{\bar{\mathbf{L}}} \left(\frac{1}{\rho} P^{n+1} \right) = \frac{2}{\Delta t} \bar{\bar{\mathbf{D}}} \mathbf{u}_{\mathcal{P}}^{n+1/2}$$

$$\frac{1}{\Delta t} \bar{\bar{\mathbf{I}}} \mathbf{u}_{\mathcal{P}}^{n+1/2} - \frac{1}{2} \bar{\bar{\mathbf{G}}} \left(\frac{1}{\rho} P^{n+1,i} \right) + \frac{1}{2} \bar{\bar{\mathbf{I}}} \mathbf{f}^{n+1} = \left(\frac{1}{\Delta t} \bar{\bar{\mathbf{I}}} - \frac{\nu}{2} \bar{\bar{\mathbf{L}}} \right) \mathbf{u}^{n+1,i+1}$$

$$v \neq 0 \text{ (iterative):} \quad \bar{\bar{\mathbf{L}}} \left(\frac{1}{\rho} P^{n+1,i} \right) = -\bar{\bar{\mathbf{D}}} \bar{\bar{\mathbf{G}}} \left(\frac{P^{n+1,i}}{\rho} \right) + \frac{2}{\Delta t} \bar{\bar{\mathbf{D}}} \mathbf{u}^{n+1,i+1}$$

SL-PFEM

Projection

Minimization of the least square error (LSE).

$\{\Psi_\lambda\}$: set of particles' values $\xrightarrow{\text{Projection}} \mathcal{P}[\{\Psi_\lambda\}] = \{\psi_c^*\}$ projected nodal values

Interpolated-projected values on particles: $\psi_h(\mathbf{X}_\lambda) = \sum_c N^c(\mathbf{X}_\lambda) \psi_c^*$

Square error: $\epsilon_\psi = \sum_\lambda (\psi_h(\mathbf{X}_\lambda) - \Psi_\lambda)^2$

$$\text{LSE: } \frac{\partial \epsilon_\psi}{\partial \psi_b^*} = 0 \rightarrow \sum_\lambda \left(\sum_c N^b(\mathbf{X}_\lambda) N^c(\mathbf{X}_\lambda) \psi_c^* \right) = \sum_\lambda N^b(\mathbf{X}_\lambda) \Psi_\lambda$$

Fulfils the coherence condition naturally

$$\Psi_\lambda = \psi_h(\mathbf{X}_\lambda) \rightarrow \epsilon_\psi = 0$$

SL-PFEM

Advantages of the SL-PFEM:

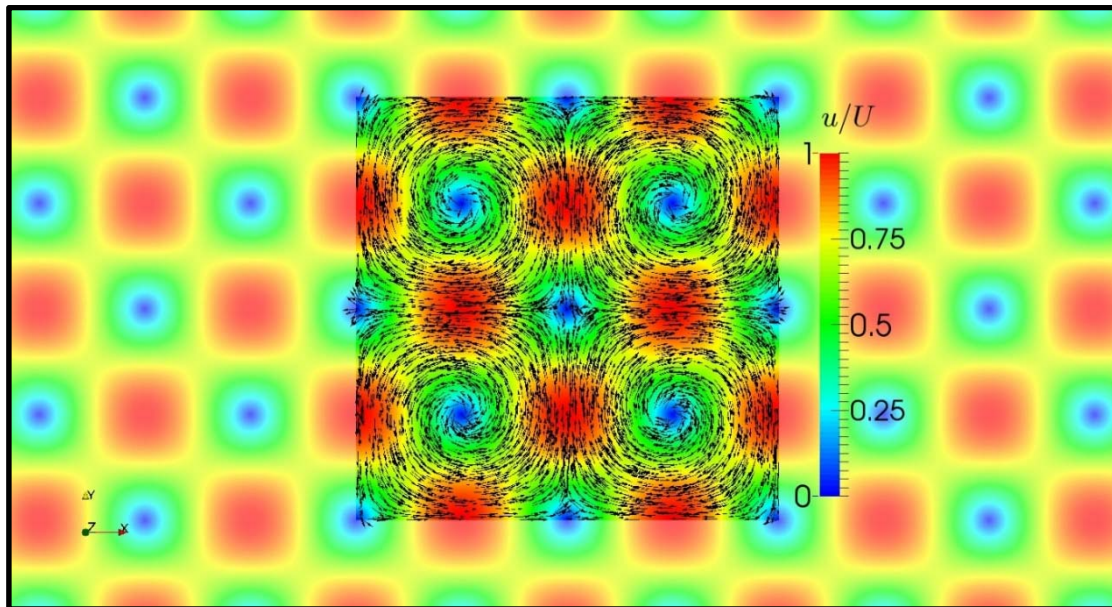
1. Explicit Lagrangian scheme for momentum equation with no stability restriction based on Courant number and low numerical erosion.
 - The time step is not limited by numerical stability. However, time step must be low enough to capture the physics. For instance, the time step must be small enough so that the particles' trajectories are accurate enough.
2. Explicit Lagrangian operations (“move particles” and “update velocity”) are embarrassingly parallel.
3. Particles can carry the information of any type of intrinsic variables.
4. FEM is very suitable to solve Stokes type equations.

VERIFICATION AND CONVERGENCE ANALYSES

TAYLOR-GREEN VORTEX

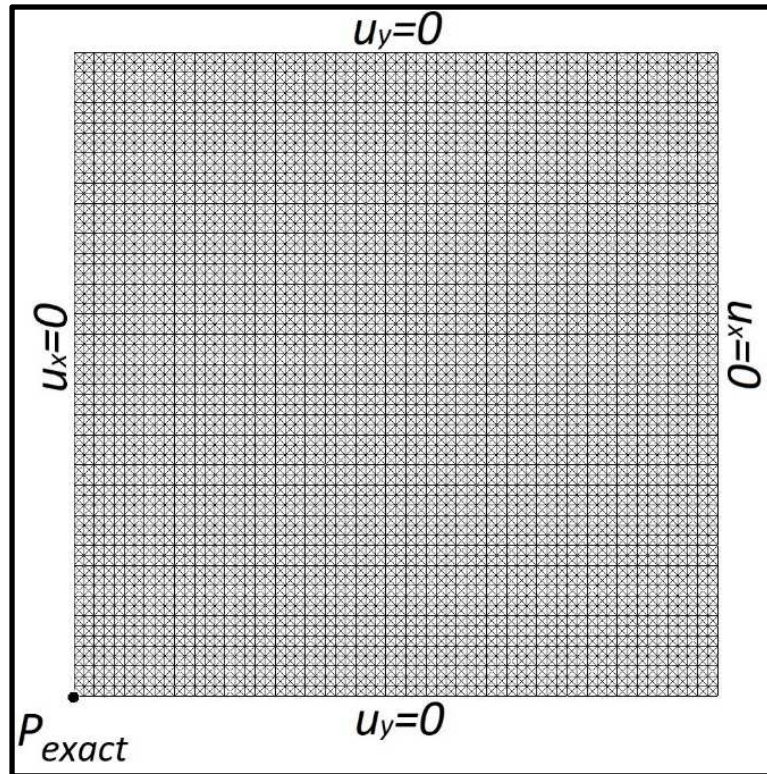
Taylor-Green vortex solution

$$\begin{aligned}u_x(x, y, t) &= -\sin(x) \cos(y) e^{-2\nu t} \\u_y(x, y, t) &= +\cos(x) \sin(y) e^{-2\nu t} \\P(x, y, t) &= \frac{1}{4} [\cos(2x) + \cos(2y)] e^{-4\nu t}\end{aligned}$$

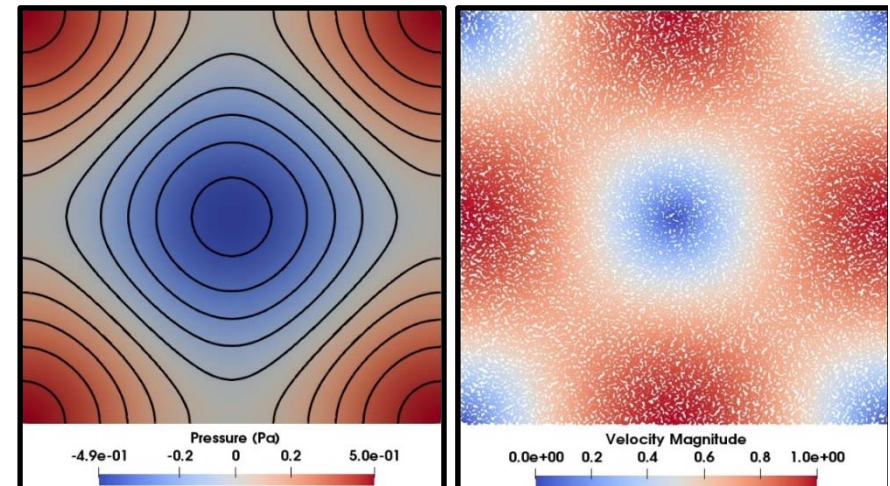


TAYLOR-GREEN VORTEX

Taylor-Green vortex decay

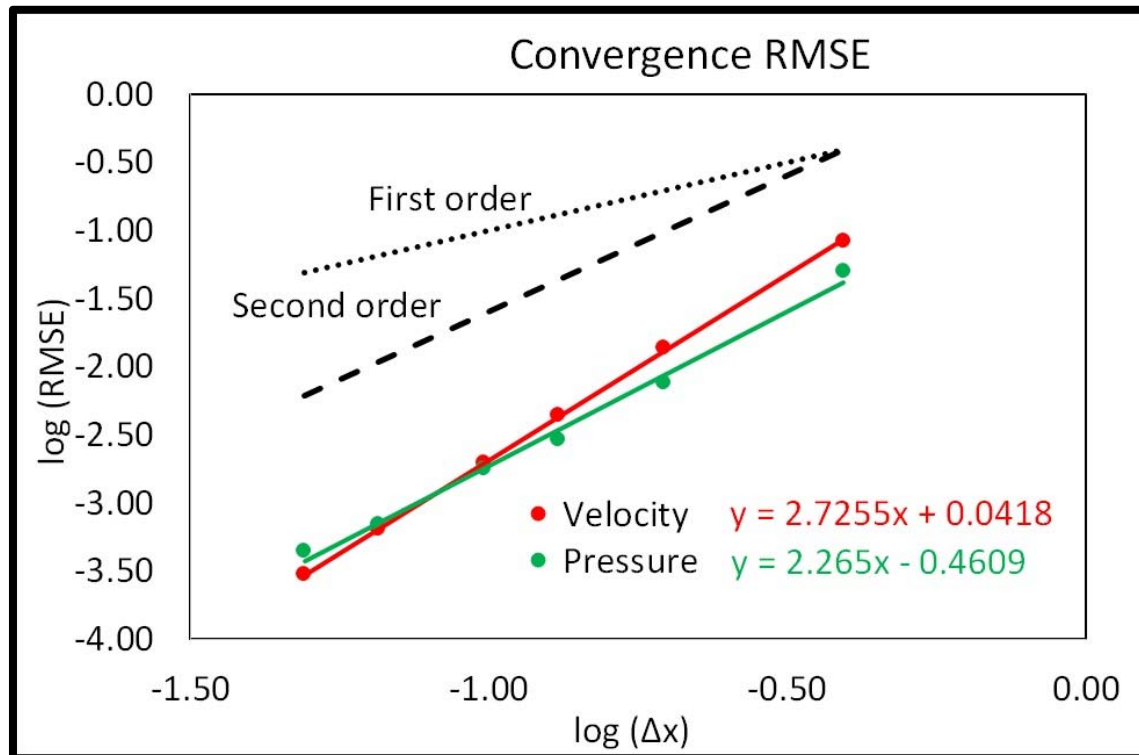


Particulars	
Maximum velocity (m/s)	1
Reynolds number	3140
Domain size (mxm)	$(0, \Pi) \times (0, \Pi)$
Courant number	0.5
Simulation time (s)	10



CONVERGENCE ANALYSIS

Taylor-Green vortex decay



Case	Δx (m)	Δt (s)	N Δt
8x8	$\pi/8$	0.2	50
16x16	$\pi/16$	0.1	100
24x24	$\pi/24$	0.0667	150
32x32	$\pi/32$	0.05	200
48x48	$\pi/48$	0.0333	300
64x64	$\pi/64$	0.025	400

CONVERGENCE ANALYSIS

Steady-state Taylor Green

Mass forces: **Vortex**

$$f_x(x, y) = -2\nu \sin(x) \cos(y)$$

$$f_y(x, y) = 2\nu \cos(x) \sin(y)$$

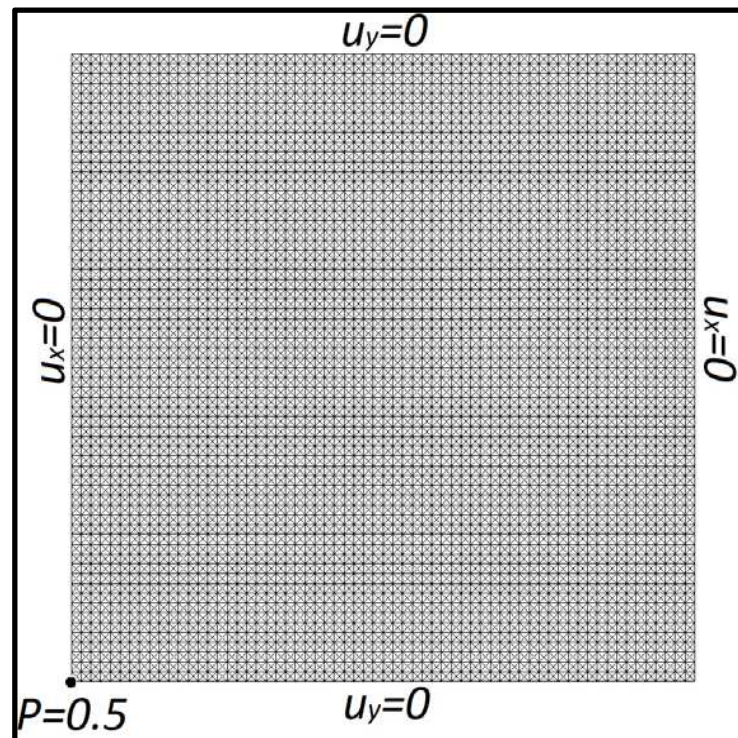
Analytical solution:

$$u_x(x, y) = -\sin(x) \cos(y)$$

$$u_y(x, y) = \cos(x) \sin(y)$$

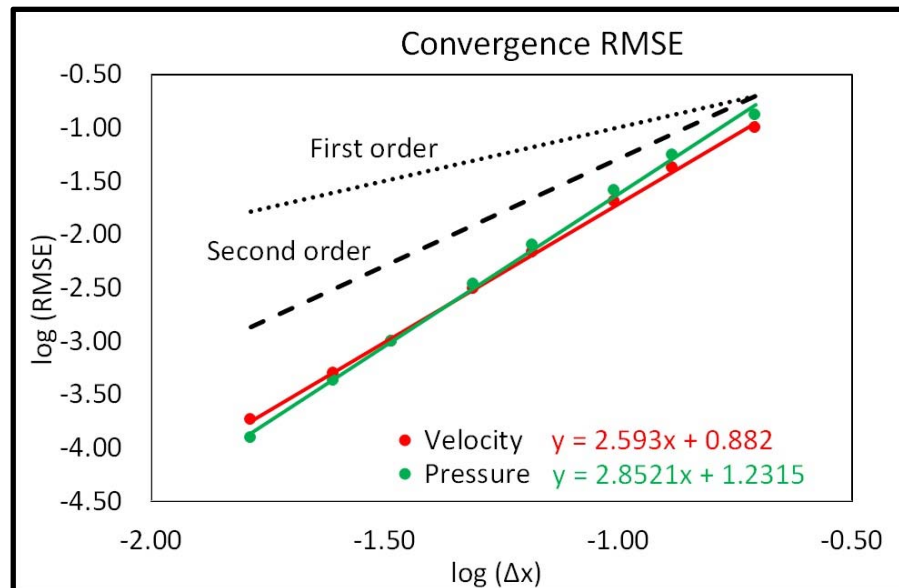
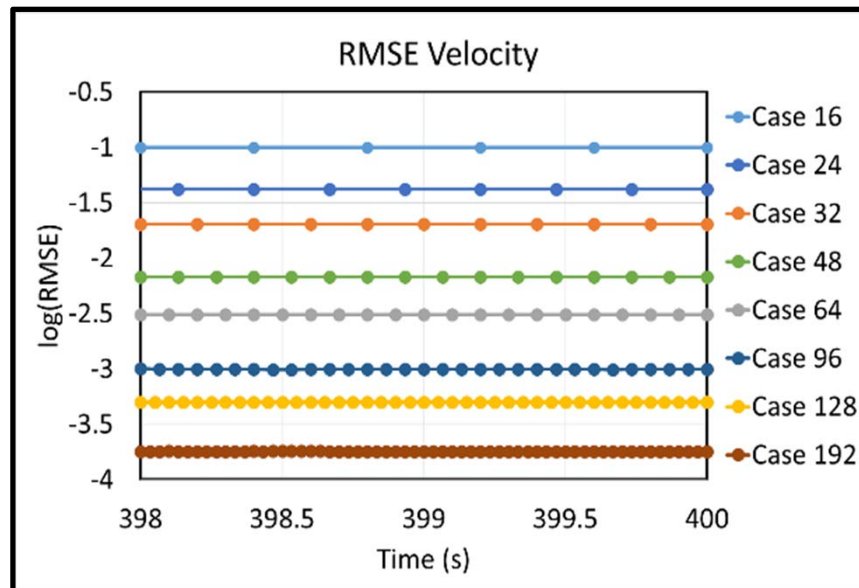
$$P(x, y) = 0.25[\cos(2x) + \cos(2y)]$$

Particulars	
Maximum velocity (m/s)	1
Reynolds number	314
Domain size (mxm)	$(0, \Pi) \times (0, \Pi)$
Courant number	2.04
Simulation time (s)	400



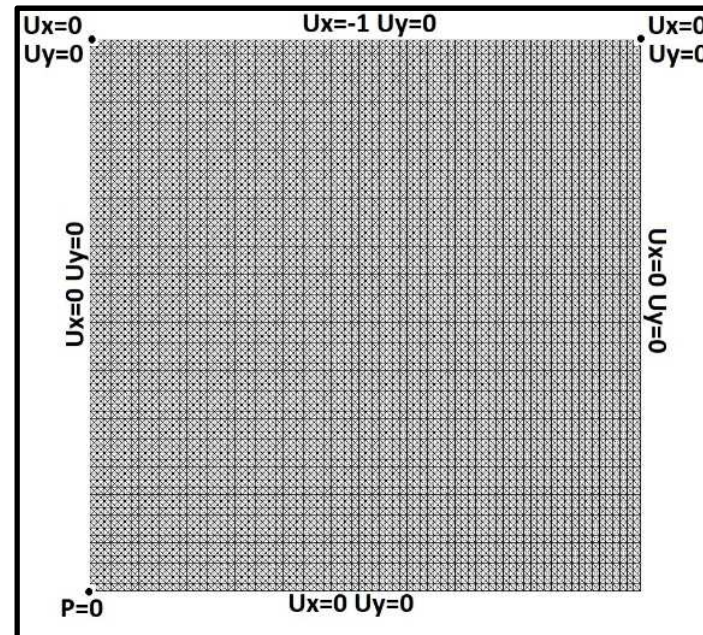
CONVERGENCE ANALYSIS

Case	$\Delta x(m)$	$\Delta t(s)$	$N \Delta t$
16x16	$\pi/16$	0.4	1000
24x24	$\pi/24$	0.2667	1500
32x32	$\pi/32$	0.2	2000
48x48	$\pi/48$	0.1333	3000
64x64	$\pi/64$	0.1	4000
96x96	$\pi/96$	0.0667	6000
128x128	$\pi/128$	0.05	8000
192x192	$\pi/192$	0.0333	12000



LID DRIVEN CAVITY FLOW

Lid velocity V	$-1m/s$
Reynolds number Re	1000
Domain size	$1m \times 1m$
Domain discretization	80×80
Number of elements	25600
Number of nodes	12961
Particles per element	3
Mesh size $\Delta x = \Delta y$	0.0125
Time step Δt	0.1
Courant number	8
Simulation time	$10^5 \Delta t$
Sampling time	$10^2 \Delta t$

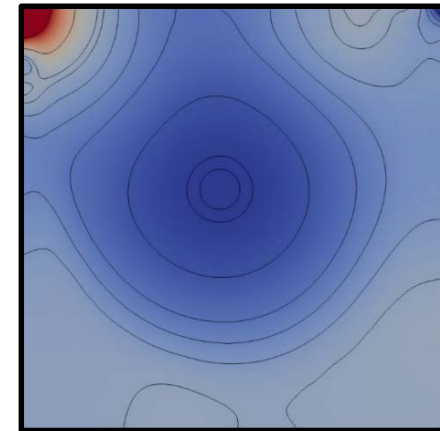
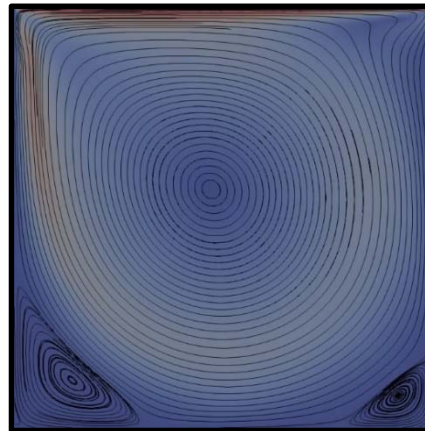


LID DRIVEN CAVITY FLOW

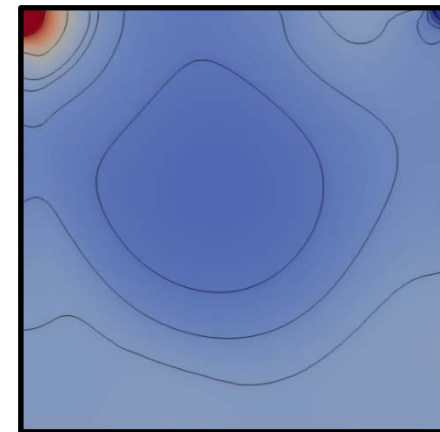
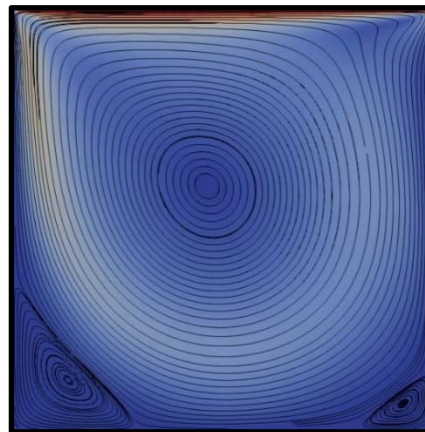
Velocity-streamlines

Pressure

Second order velocity
Verlet SL-PFEM



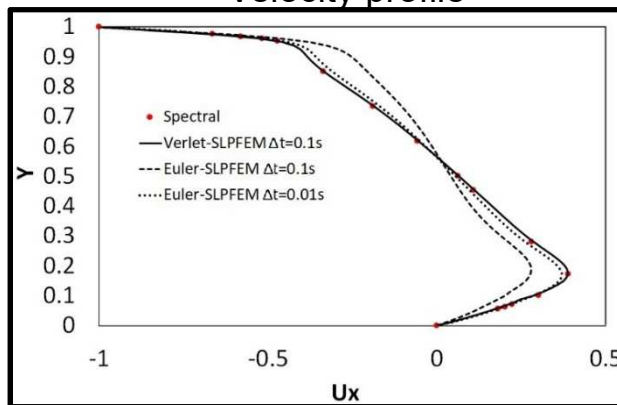
First order
Euler SL-PFEM



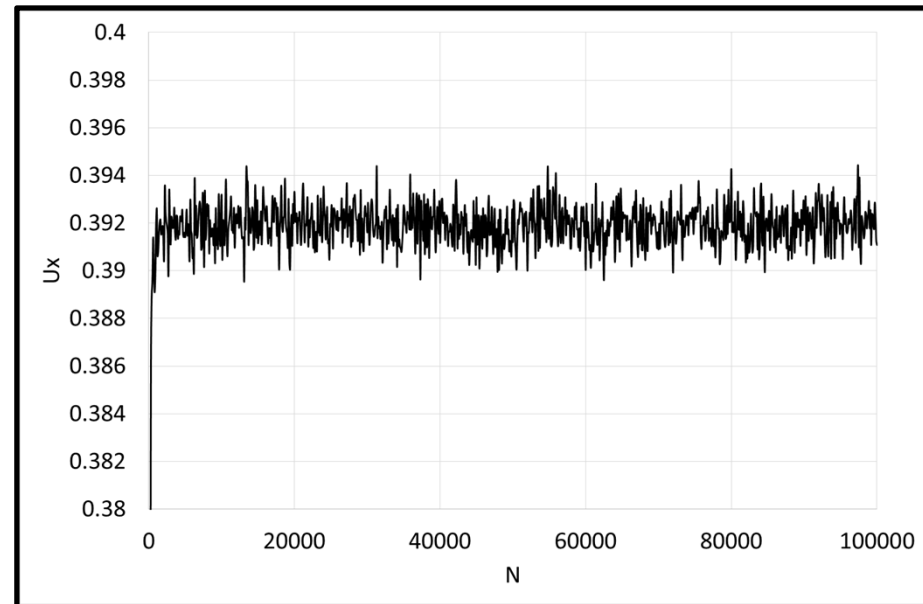
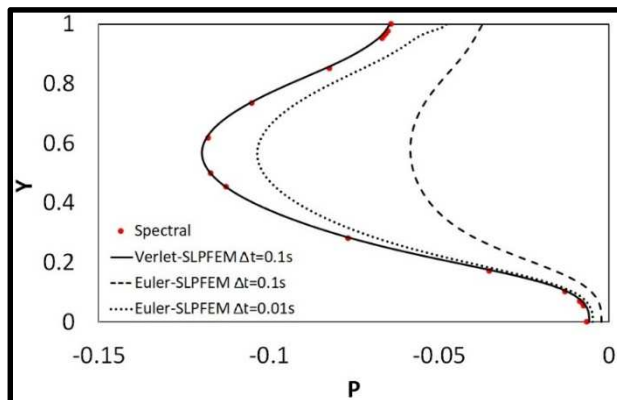
LID DRIVEN CAVITY FLOW

Horizontal velocity and pressure profiles at the mid-section $x=0.5$. Solid line: Second Order Verlet-SLPFEM. Dash line: First Order in time Euler-SLPFEM. Red dots: spectral method (O. Botella and R. Peyret. Benchmark spectral results on the lid-driven cavity flow. Computers & Fluids Vol. 27, No. 4, pp. 421-433, 1998)

Velocity profile



Pressure profile

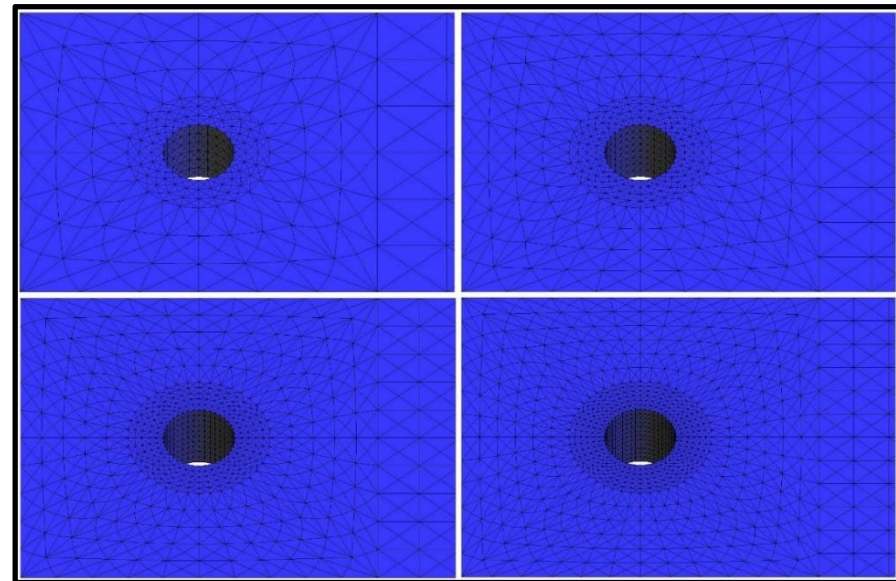


Horizontal velocity evolution at $(x,y)=(0.5,0.175)$
for the second-order Verlet -SLPFEM

3D FLOW PAST A CYLINDER

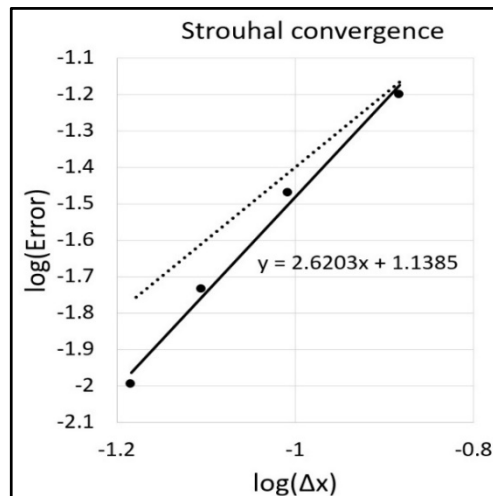
Mesh	$\Delta x(m)$	$\Delta t(s)$	N tetras	N Nodes	N Δt
1	0.1333	0.0667	62208	14487	1500
2	0.1	0.05	147456	33412	2000
3	0.08	0.04	288000	64185	2500
4	0.0667	0.0333	497664	109686	3000

Particulars	
Cylinder diameter (m)	1
Cylinder height (m)	1
Inlet velocity (m/s)	1
Reynolds number	200
Courant number	2

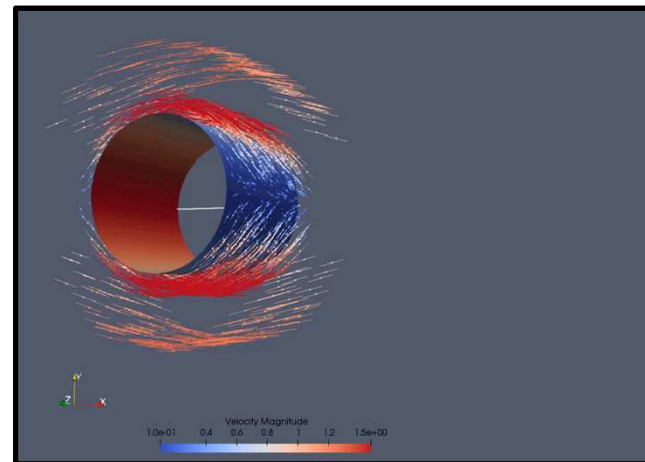


3D FLOW PAST A CYLINDER

Case	St	Error St	C_L
1	0.133	0.0630	0.177
2	0.162	0.0339	0.255
3	0.178	0.0184	0.246
4	0.186	0.0101	0.258
Ref. [*]	0.196		



CPU time in seconds per time step (mesh 2)			SL-PFEM		FEM
Particles	Move		0.092	0.602	
	Projector	Assembly	0.363		
		Solver	0.147		
Velocity solver			0.125		1.532
Pressure solver			0.339		0.320
Total			1.066		1.852



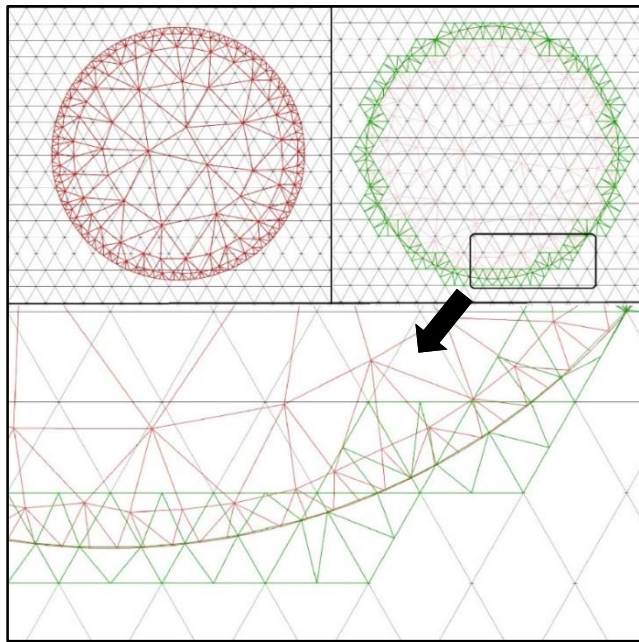
* H. Jiang and L. Cheng. Strouhal Reynolds number relationship for flow past a circular cylinder. J. Fluid Mech. (2017), vol. 832, pp. 170-188

ENRICHED SL-PFEM

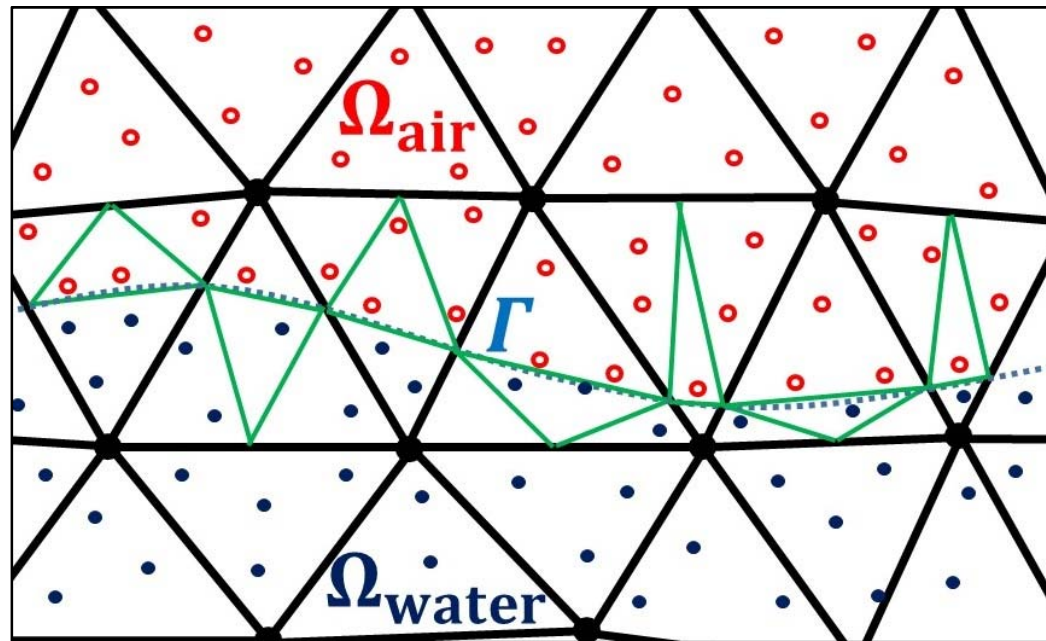
ENRICHMENT

Based on local refinement and the introduction of new degrees of freedom at the interface

Fluid-Solid:



Free Surface:



ENRICHMENT

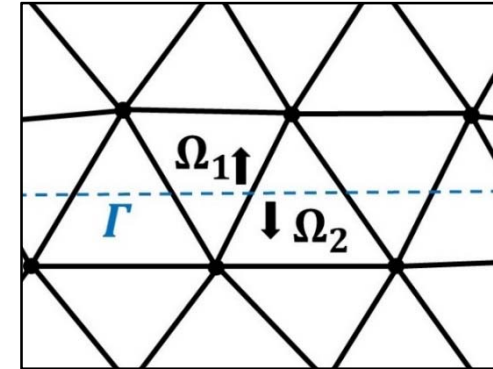
Pressure Enrichment:

Governing Eq: $\Delta P_f = \rho_f \nabla \cdot \mathbf{u}_p$

BC: $\frac{1}{\rho_{f1}} \nabla P_{f1} \cdot \mathbf{n}_\Gamma = \frac{1}{\rho_{f2}} \nabla P_{f2} \cdot \mathbf{n}_\Gamma$ on Γ

Variational formulation:

$$\int_{\Omega_f} \omega \Delta P_f d\Omega_f = - \int_{\Omega_f} \nabla \omega \nabla P_f d\Omega + \int_{\Gamma_f} \omega (\nabla P_f \cdot \mathbf{n}) d\Gamma_f = \rho_f \int_{\Omega_f} \omega (\nabla \cdot \mathbf{u}_p) d\Omega_f$$



FEM matrix system of equations: $\bar{\bar{\mathbf{K}}}_f \mathbf{P}_f = \bar{\bar{\mathbf{D}}} \cdot \mathbf{u}_p - (\bar{\bar{\mathbf{D}}}_f + \bar{\bar{\mathbf{D}}}_f^T) \cdot \bar{\bar{\mathbf{G}}}_f \mathbf{P}_f$

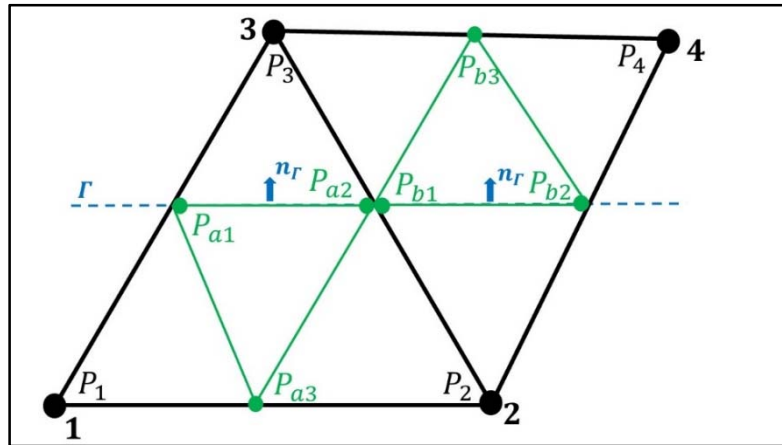
where

$$\bar{\bar{\mathbf{K}}}_f = -\frac{1}{\rho_f} \left[\int_{\Omega_f} \nabla N^i \nabla N^j d\Omega_f \right] \quad \bar{\bar{\mathbf{G}}}_f = \frac{1}{\rho_f} \int_{\Omega_f} N^i \nabla N^j d\Omega_f / \int_{\Omega_f} N^i d\Omega_f$$

$$\bar{\bar{\mathbf{D}}}_f = \int_{\Omega_f} N^i \nabla N^j d\Omega_f \quad \bar{\bar{\mathbf{D}}}_f^T = \int_{\Omega_f} \nabla N^i N^j d\Omega_f$$

$$(\bar{\bar{\mathbf{D}}}_f + \bar{\bar{\mathbf{D}}}_f^T) \cdot \bar{\bar{\mathbf{G}}}_f \mathbf{P}_f = \left[\int_{\Gamma_f} N^i N^j \mathbf{n} d\Gamma_f \right] \cdot \bar{\bar{\mathbf{G}}}_f \mathbf{P}_f$$

ENRICHMENT



Enriched matrix:

K_{11}	K_{22}	K_{33}	K_{44}	KA_{11}	0	KA_{13}	0	0	0
				0	KA_{22}	KA_{23}	KB_{21}	KB_{22}	0
				KA_{31}	0	KA_{33}	KB_{31}	0	KB_{33}
				0	0	0	0	KB_{42}	KB_{43}
$\bar{K}\bar{A}^T$				A_{11}	A_{12}	A_{13}	$\bar{0}$		
				A_{21}	A_{22}	A_{23}			
				A_{31}	A_{32}	A_{33}			
$\bar{K}\bar{B}^T$				$\bar{0}$			B_{11}	B_{12}	B_{13}
							B_{21}	B_{22}	B_{23}
							B_{31}	B_{32}	B_{33}

Interpolate:

$$\nabla \bar{P}_{a2} = \nabla \bar{P}_{b1} = \text{Interp}(\nabla \bar{P}_2, \nabla \bar{P}_3)$$

$$\mathbf{u}_{a2} = \mathbf{u}_{b1} = \text{Interp}(\mathbf{u}_2, \mathbf{u}_3)$$

Enriched system:

$$\begin{bmatrix} \bar{I}_K & \bar{K}\bar{A} & \bar{K}\bar{B} \\ \bar{K}\bar{A}^T & \bar{A} & \bar{0} \\ \bar{K}\bar{B}^T & \bar{0} & \bar{B} \end{bmatrix} \begin{bmatrix} P \\ P_A \\ P_B \end{bmatrix} = \begin{bmatrix} rhs \\ rhs_A \\ rhs_B \end{bmatrix}$$

Collapse enriched nodes: $P_A = \bar{A}^{-1}(rhs_A - \bar{K}\bar{A}^T P)$ $P_B = \bar{B}^{-1}(rhs_B - \bar{K}\bar{B}^T P)$

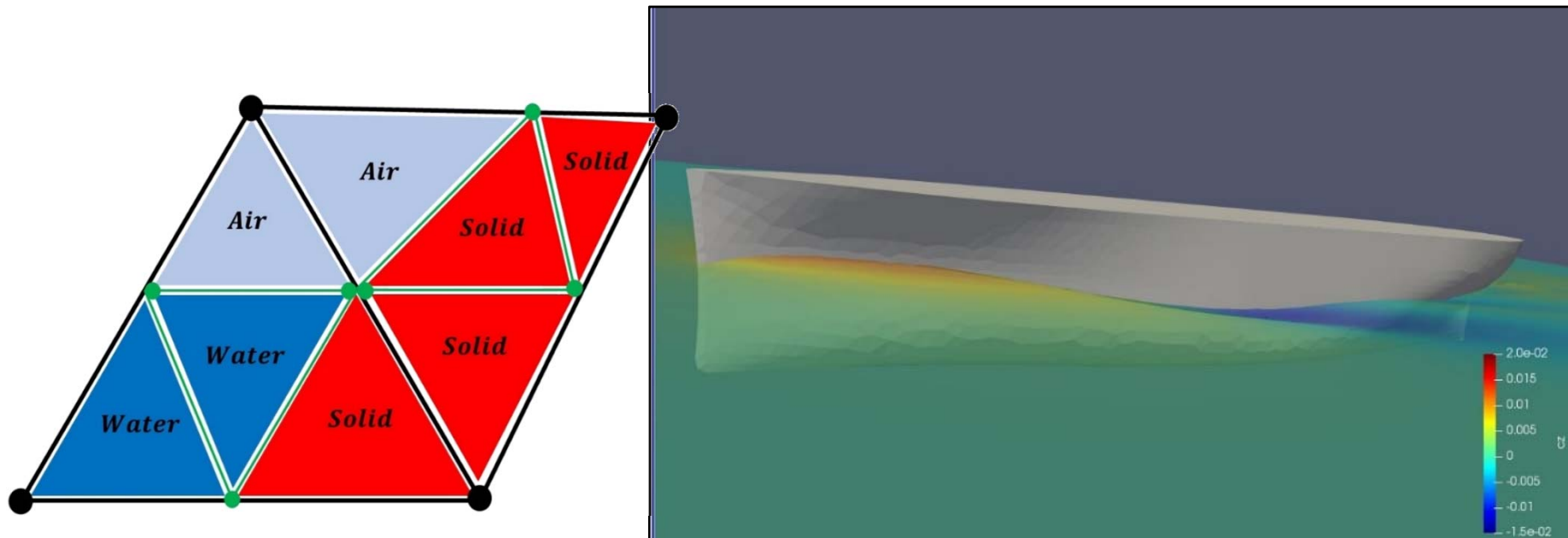
New pressure system: $[\bar{I}_K - \bar{K}\bar{A} \bar{A}^{-1} \bar{K}\bar{A}^T - \bar{K}\bar{B} \bar{B}^{-1} \bar{K}\bar{B}^T][P] = [rhs - \bar{K}\bar{A} \bar{A}^{-1} rhs_A - \bar{K}\bar{B} \bar{B}^{-1} rhs_B]$

ENRICHMENT

Velocity Enrichment for solid fluid interface:

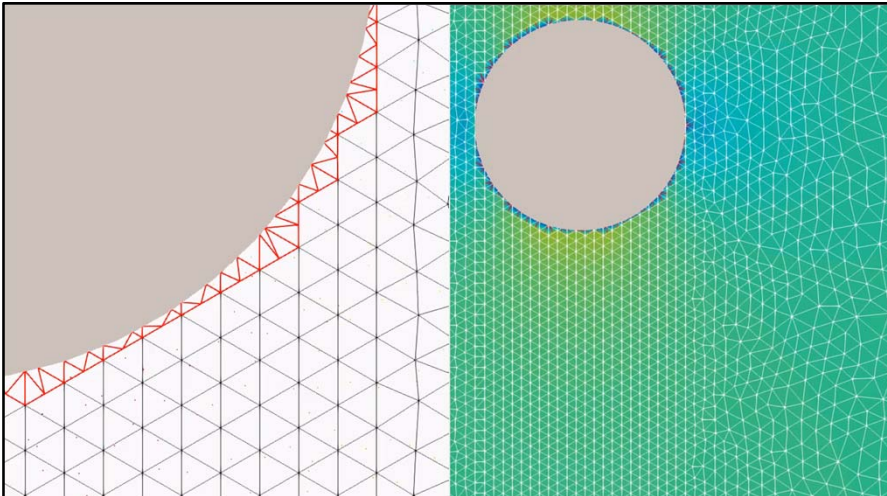
$$\text{New velocity system: } [\bar{I}_K][U] = [rhs - \bar{K}\bar{A} U_A - \bar{K}\bar{B} U_B]$$

Water-Air-Solid interfaces:

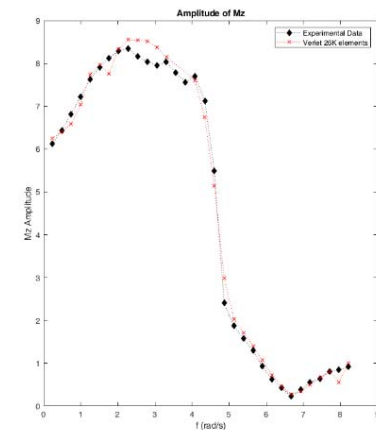
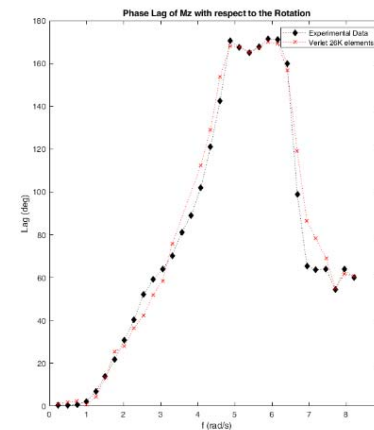
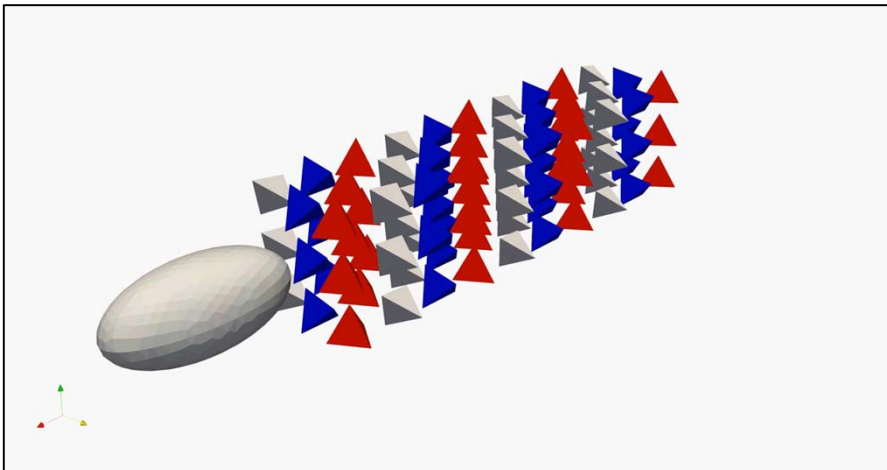
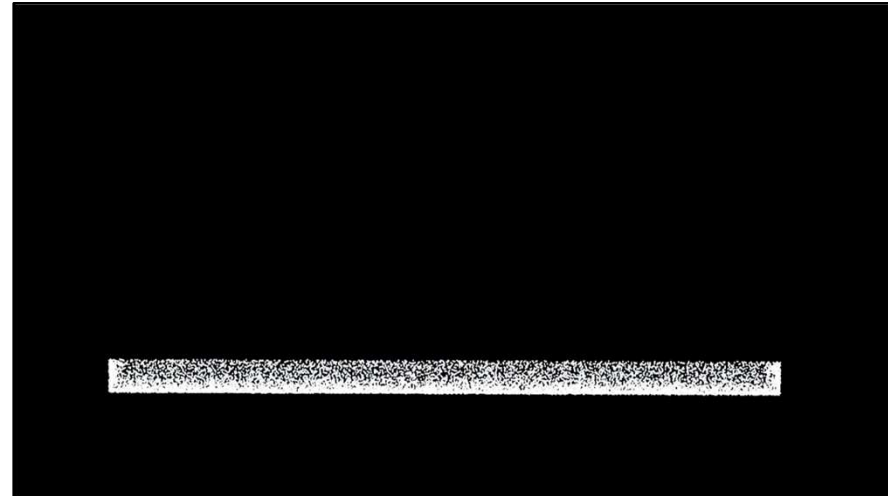


ENRICHMENT + BODY DYNAMICS + CONTACTS

Fluid-Solid interface:



Water-Air interface:

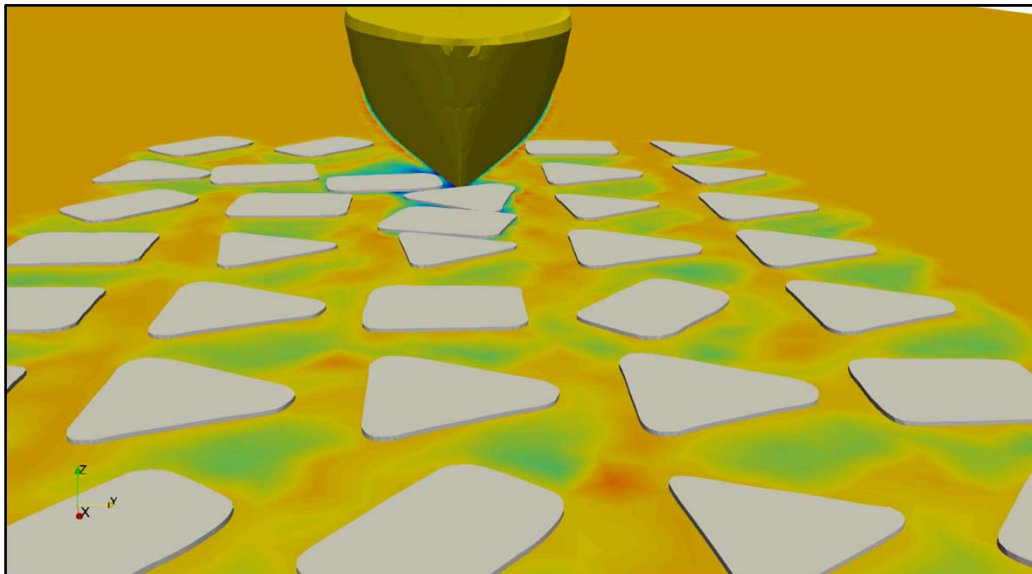


ONGOING AND FUTURE WORK RESEARCH LINES

ONGOING WORK

Ship navigation in ice conditions (NICESHIP project):

- Development of the SL-PFEM for high fidelity simulations of a ship navigating in ice conditions.
- Towing tank tests are being carried out at the ETSIN-UPM.
 - Paraffin wax is used to simulate ice.
 - The Hespérides hull will be analyzed.



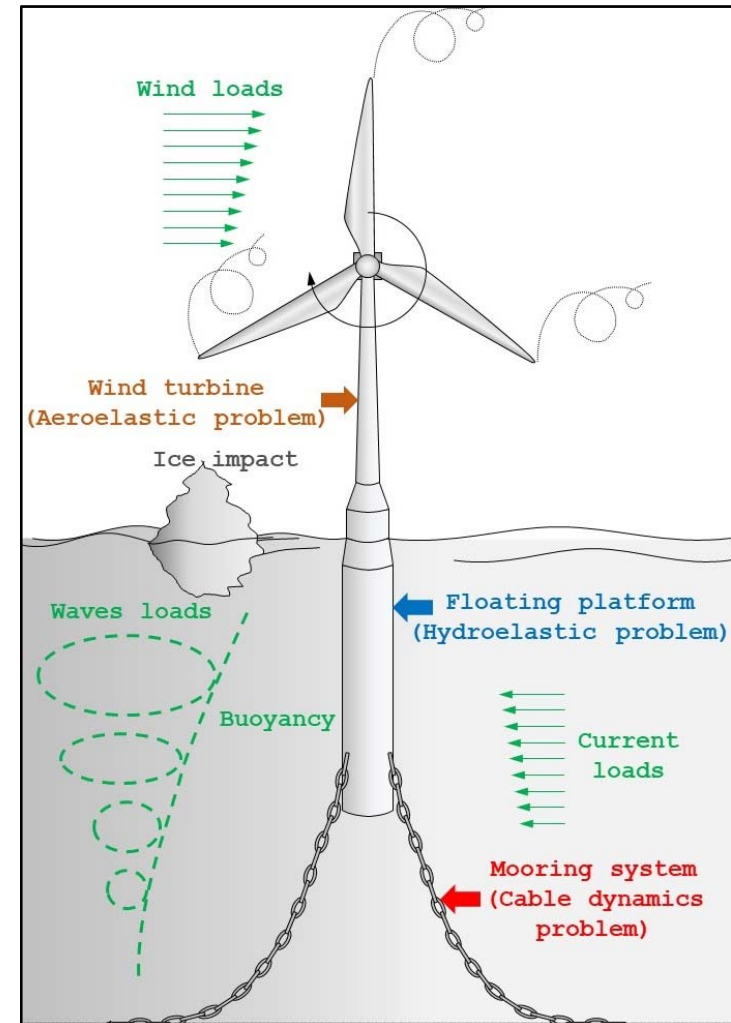
ONGOING WORK

Simulation of Floating Offshore Wind Turbines (FOWT):

- Tailoring the SL-PFEM for high fidelity simulation of seakeeping hydrodynamics.
- Coupling the SL-PFEM with:
 - OpenFAST (Aerolasticity)
 - Structural solver (in house)
 - Mooring solver (in house).
- Development of Structural Reduced Order Models
- Development of Virtual twin for structural health monitoring.

References:

- Servan-Camas, B., Gutierrez-Romero, J. E., and Garcia-Espinosa, J. *A time-domain second-order FEM model for the wave diffraction-radiation problem. Validation with a semisubmersible platform.* Marine Structures. 58, pp. 278 - 300. Elsevier, 2018.
- Gutierrez-Romero, J. E., Garcia-Espinosa, J., Servan-Camas, B., and Zamora-Parra, B. *Non-linear dynamic analysis of the response of moored floating structures.* Marine Structures. 49, pp. 116 - 137. Elsevier, 2016.



FUTURE WORK

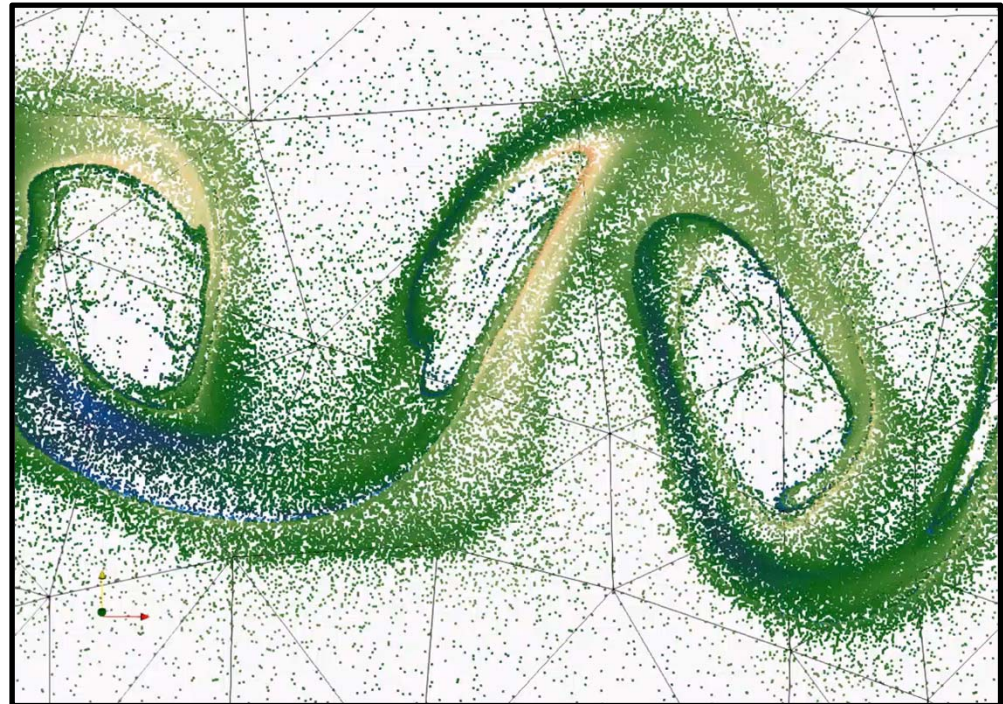
FUTURE WORK

Future Work

- ✓ Resolve subgrid scales
 - ✓ Solve particle scale vorticity using a particle based vortex method.
- ✓ Lagrangian approach for turbulence modelling
- ✓ Create computational framework for Multiphysics problems.

References

- Jonathan Colom-Cobb, Julio Garcia-Espinosa, Borja Servan-Camas & P. Nadukandi. *A second-order semi-Lagrangian particle finite element method for fluid flows*. Comp. Part. Mech. DOI 10.1007/s40571-019-00258-9
- Nadukandi, P., Servan-Camas, B., Becker, P. A., and Garcia-Espinosa, J. *Seakeeping with the semi-Lagrangian Particle Finite Element Method*. Computational Particle Mechanics. Springer, 2016.



ACKNOWLEDGEMENTS

The authors acknowledge Office of Naval Research Global for supporting this work. This work relates to Department of the Navy Grant N62909-16-1-2236 issued by Office of Naval Research Global.

Support for this research provided by the project NICESHIP RTI2018-094744-B-C21 of the Ministry of Science and Innovation of Spain is also gratefully acknowledged.